

Quality Assessment of the Cobel-Isba Numerical Forecast System of Fog and Low Clouds

THIERRY BERGOT

Abstract—Short-term forecasting of fog is a difficult issue which can have a large societal impact. Fog appears in the surface boundary layer and is driven by the interactions between land surface and the lower layers of the atmosphere. These interactions are still not well parameterized in current operational NWP models, and a new methodology based on local observations, an adaptive assimilation scheme and a local numerical model is tested. The proposed numerical forecast method of foggy conditions has been run during three years at Paris-CdG international airport. This test over a long-time period allows an in-depth evaluation of the forecast quality. This study demonstrates that detailed 1-D models, including detailed physical parameterizations and high vertical resolution, can reasonably represent the major features of the life cycle of fog (onset, development and dissipation) up to +6 h. The error on the forecast onset and burn-off time is typically 1 h. The major weakness of the methodology is related to the evolution of low clouds (stratus lowering). Even if the occurrence of fog is well forecasted, the value of the horizontal visibility is only crudely forecasted. Improvements in the microphysical parameterization and in the translation algorithm converting NWP prognostic variables into a corresponding horizontal visibility seems necessary to accurately forecast the value of the visibility.

Key words: Numerical prediction, fog, short term forecast.

1. Introduction

Air-traffic safety and operational efficiency depend heavily upon accurate and timely forecasts of fog and low clouds. Adverse visibility conditions can strongly reduce the efficiency of terminal area traffic flow. For example, at Paris - Charles de Gaulle international airport (Paris-CdG), the landings and departures are reduced by a factor of 2 in foggy conditions (so called *Low Visibility Procedures (LVP)*, defined by Air Traffic Control authorities (ATC) and corresponding to visibility < 600 m or ceiling < 200 ft -about 60 m). The occurrence of poor visibility conditions restricting the flow of air traffic in major airport terminals is one of the main causes of aircraft delays. Accurate anticipation of the onset and cessation of LVP conditions allows for air-traffic managers to effectively regulate traffic and to optimize the use of airport capacity.

GAME-CRNM (Météo-France, CNRS) Centre National de Recherches Météorologiques, 42, avenue G. Coriolis, F-31057, Toulouse cedex, France. E-mail: Thierry.Bergot@meteo.fr

Land surface and boundary layer processes play a fundamental role in the life cycle of a fog layer. These effects are still not well parameterized in current operational numerical weather prediction (NWP) models. Moreover, horizontal and vertical resolution of the current NWP models are larger than the corresponding characteristic fog scales (TARDIF, 2007). Consequently, fog and low clouds that are predominantly driven by local influences are poorly forecast by current NWP models. Single-column models are able to overcome these deficiencies, despite the poor estimate of horizontal heterogeneities. Several 1-D models have been used to study fog layers (e.g., MUSSON-GENON, 1986; DUYNKERKE, 1991; BERGOT and GUÉDALIA, 1994). Moreover, 1-D models are currently used in real time to forecast fog at the local scale (CLARK, 2002, 2006; TERRADELLAS and CANO, 2003; TERRADELLAS *et al.*, 2005; HERZEGH *et al.*, 2003). These feasibility studies have demonstrated the capabilities of local numerical models for short-term forecasting. Moreover, it is obvious that an important component for success is the capacity to initialize at their best, the local numerical model using specific observations and a local adaptive assimilation scheme (BERGOT *et al.*, 2005). The methodology tested in this article is based on Cobel-Isba numerical prediction system operationally used at Paris-CdG airport to forecast LVP conditions.

The objective of the work presented here is to evaluate the performance of the Cobel-Isba numerical prediction system used at Paris-CdG airport over a period of three years. This evaluation aims to better identify the strengths and weaknesses of the system, and facilitate an optimal use of Cobel-Isba forecast products. A brief description of the numerical method, including local assimilation and Cobel-Isba numerical model, is presented in section 2. The quality of the forecast of LVP conditions at Paris-CdG is detailed in section 3. Finally, recommendations and the limitation of this kind of local numerical modelling are outlined in section 4.

2. Numerical Forecast System

a. Cobel-Isba Numerical Model

The atmospheric model used in this study is the high resolution 1-D Cobel (Code de Brouillard à l'échelle locale) model. This column model was developed in collaboration between the Laboratoire d'Aérodynamique (Université Paul Sabatier/C.N.R.S., France), Université du Québec à Montréal (U.Q.A.M., Canada) and Centre National de Recherches Météorologiques (GAME-CNRM/CNRS, France). A detailed description can be found in BERGOT (1993), BERGOT and GUÉDALIA (1994), and only a brief description will be given hereafter.

The model equations are classically derived from the Boussinesq hypothesis, under the assumption of horizontal homogeneity. However, spatial heterogeneities are treated as an external mesoscale forcing and are evaluated from the Météo-France operational NWP model Aladin (model grid box of about 10 km). These mesoscale

forcings (horizontal advection of temperature, horizontal advection of water vapor, vertical velocity, geostrophic wind and cloud cover), varying with time and height, are used to modify the thermodynamic evolution of the boundary layer.

The Cobel model equations are solved on a high resolution vertical grid: Near the surface, typical region for fog and very low clouds (i.e., below 200 m), numerical computations are made on 20 vertical levels (the first level is at 50 cm). The main characteristics of the physical package used in the Cobel model are described below. It includes a parameterization of boundary layer turbulent mixing, an explicit cloud scheme and parameterizations of longwave and shortwave radiation transfer.

The Cobel model is coupled with the multi-layer surface: vegetation-atmosphere transfer scheme, ISBA—Interactions Soil Biosphere Atmosphere—(NOILHAN and PLANTON, 1989; BOONE, 2000; BOONE *et al.*, 1999). The ISBA surface scheme describes the interactions between the land surface and the overlying atmosphere. In this study, seven soil layers are used to represent a soil column of 2 m in depth. The thickness of the first soil layer is 0.5 cm and the thickness is of 2.5 cm for the second soil layer.

1) *Turbulence scheme*

The turbulent exchanges inside the boundary layer are treated using a 1.5-order turbulence closure scheme. The turbulent fluxes are parameterized using a predictive equation for the turbulent kinetic energy (TKE) and the mixing length is a function of the stability of the atmosphere. For stable stratification, the mixing length is a function of the Richardson number, following ESTOURNEL and GUÉDALIA (1987). For unstable stratification, the mixing length follows BOUGEAULT and LACARRERE (1989).

2) *Microphysics*

The cloud liquid water content q_l is computed as a prognostic variable, and the size distribution of the droplets is not considered. The parameterization of the gravitational settling flux of cloud droplets is related to the liquid water content by way of a settling velocity, v_i (BROWN and ROACH, 1976). A constant value of $v_i = 1.6 \text{ cm s}^{-1}$, derived from observations of fog droplet size distributions, is used in this study.

Following KUNKEL (1984), the visibility is deduced from the liquid water content

$$\text{visibility (m)} = \frac{3.9}{144.7(\rho q_l)^{0.88}}. \quad (1)$$

3) *Radiation*

The longwave radiation parameterization is a high resolution spectral scheme that computes the longwave radiation fluxes at every model level for 232 spectral intervals between 4 μm and 100 μm (VEHIL *et al.*, 1989). The radiative effect of the droplets is calculated inside the atmospheric window by relating linearly the longwave optical depth to the liquid water content.

The shortwave radiation is computed following the mono-spectral scheme of FOUQUART and BONNEL (1980). The effect of cloud droplets is parameterized by computing the shortwave optical thickness which is related to the liquid water content. The single scattering albedo of fog and low cloud is related to the optical thickness.

b. Assimilation Scheme

Accurate short-term forecasting of local conditions, including low ceiling and poor visibility, strongly depends on the accuracy of the initial conditions. Specific measurements have been obtained at Paris-CdG since December 2002 in order to improve the description of the surface boundary layer. These specific measurements can be summarized by

- a 30-m meteorological tower collecting observations of temperature and humidity at 1 m, 2 m, 5 m, 10 m and 30 m;
- the divergence of the radiation fluxes estimated following shortwave and longwave radiation fluxes measured at the ground level and at 45 m;
- soil temperature and soil moisture measured at -5 cm, -10 cm, -20 cm, -30 cm and -50 cm in depth.

The assimilation procedures associated with Cobel-Isba and used to construct the initial conditions are as follows:

- to estimate the atmospheric vertical profile of temperature and humidity in a 1-D-Var framework;
- if low clouds or fog are detected, adjustments of the atmospheric profiles are introduced to take into account the presence of clouds;
- to estimate the vertical profiles of temperature and water content within the soil.

A detailed description and validation of this local assimilation scheme can be found in BERGOT *et al.* (2005), and only a brief description will be given hereafter.

1) Assimilation of atmospheric profiles: 1-D-Var

The estimation of the initial profiles uses a variational assimilation approach. Observational errors are assumed to be uncorrelated. The error statistics are imposed arbitrarily but allow the initial profile to be very close to the observations near the surface, and to get closer to the 3-D NWP forecast above the boundary layer (see BERGOT *et al.*, 2005 for details).

2) Assimilation of fog and low clouds layer

The following procedure is used to modify the initial profile of temperature and humidity when fog or low clouds are detected. The main goal is to accurately represent the atmospheric boundary layer structure inside the fog layer.

It is now well known that mature fog is a well-mixed atmospheric layer as a consequence of the profile of radiative divergence. Consequently, the atmospheric profiles inside the fog or low cloud layer are adjusted following the hypothesis that total water content (liquid and vapor) is constant, that the temperature follows a moist adiabatic profile, and that the atmosphere is saturated. Above the fog or low cloud layer, the atmospheric profiles from the 1-D-Var system are not modified.

The fog depth is determined using an iterative method with the goal of minimizing the model error on radiation flux divergence. If the fog or low clouds layer is above the upper level of measurement (about 25% of studied cases), the vertical gradient between the two levels of radiative measurements is about zero, and the methodology previously presented will not be applicable. In this case, the fog depth is determined by minimizing the error on the shortwave radiation at the ground during the day or by minimizing the error on longwave radiation at the ground during the night.

3) *Assimilation of soil profiles*

The temperature and moisture profiles are linearly interpolated from *in situ* measurements.

3. *Forecast Quality*

The Cobel-Isba numerical prediction system has been run for three years, every 3 h at 00UTC, 03UTC, 06UTC, 09UTC, 12UTC, 15UTC, 18UTC and 21UTC (local time = UTC + 1 during the winter season). The forecast has been performed up to +12 h. The occurrence of LVP conditions is defined every 30 minutes for both observations and forecasts. An observed or forecast LVP event was considered when the ceiling was less than 200 ft (about 60 m) or the visibility less than 600 m. The Cobel-Isba forecasts are matched against observations. Overall verification statistics are calculated based on binary LVP / no-LVP categories. The statistics produced are based on the hit ratio (HR) and false alarm rate (FAR). If a is the number of observed and forecast events, b the number of *not* observed and forecast events, and c the number of observed and *not* forecast events, these scores are determined by:

$$\begin{aligned} \text{HR} &= \frac{a}{a+c}, \\ \text{FAR} &= \frac{b}{a+b}. \end{aligned} \tag{2}$$

a. Verification Statistics

The frequency distribution histogram of LVP conditions along a diurnal time scale is plotted in Figure 1a for observations and in Figure 1b for all Cobel-Isba

forecasts (including all forecasted time and all runs). The relative distribution of LVP conditions is globally well forecasted by the Cobel-Isba model, with a maximum of occurrence at the end of the night and a minimum during the afternoon. However, some difference appears at the beginning of the night and at the end of the night. Between 03UTC and 06UTC, the Cobel-Isba model over-forecasts the occurrence of LVP conditions, with a maximum of 7.45% at 06UTC instead of 6.98% for observations. The sharp decrease of LVP conditions observed between 08UTC (7.45%) and 09UTC (5.43%) is slightly delayed for the Cobel-Isba forecasts between 09UTC (6.53%) and 10UTC (4.68%). At the beginning of the night, between 17UTC and 20UTC, the Cobel-Isba model under-forecasts the occurrence of LVP condi-

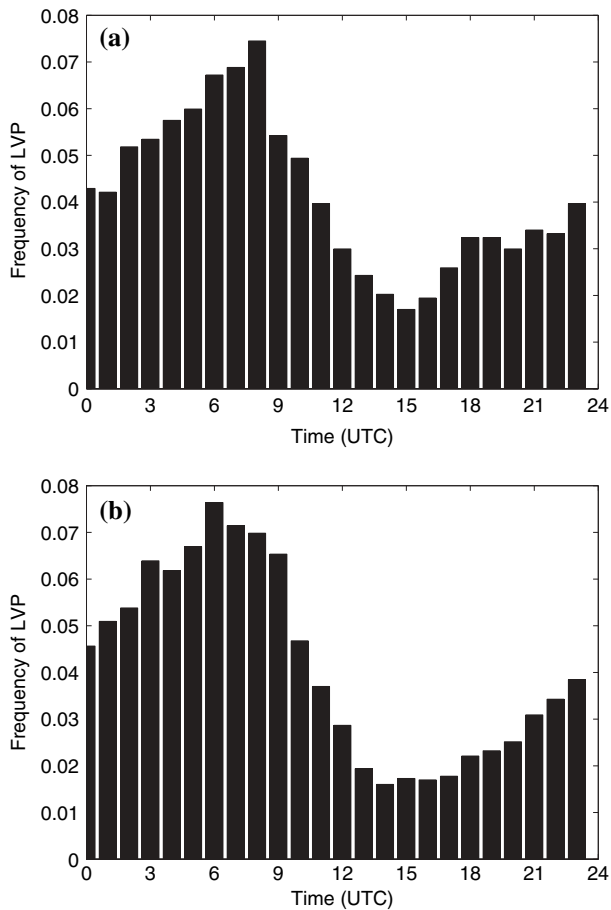


Figure 1

Frequency distribution histogram of the occurrence of LVP conditions as a function of daytime for observation (a), Cobel-Isba forecasts (b).

tions. For example, at 18UTC, the observed occurrence is 3.21% and the forecasted occurrence is 2.21%.

Figure 2 shows the time evolution of the hit ratio (HR) and false alarm rate (FAR) for the Cobel-Isba forecasts up to +12 h. During the first 3 h of simulation the evolution is marked, FAR sharply increases and reaches 0.55 while HR decreases and reaches 0.60. HR is larger than FAR until +4 h forecast time. Afterwards, FAR increases very slowly to reach 0.67 for +12 h forecast while HR decreases to reach 0.32 for +12 h forecast. To examine the dependence of the forecast skill as a function of the initialization time, the statistics are presented for the various initialization times: Table 1 for +1 h forecast, Table 2 for +2 h forecast and Table 3 for +6 h forecast. The worst forecasts occur when the model is initialized during the daytime (typically 12UTC). During daytime, the local impact of observations in the surface boundary layer lasts only a few minutes since 3-D turbulence and mesoscale advections are expected to play a predominant role. However, the number of LVP events is small during this time period. The best results are obtained when the model is initialized at 03UTC, 06UTC and 21UTC. At the end of the night, an accurate initialization of fog and low clouds is crucial to forecast the evolution of the atmosphere close to the surface (e.g., BERGOT *et al.*, 2005). The score of the Cobel-Isba forecasts at sunrise demonstrates the quality of the initialization scheme including the specific observations. The decrease of the forecasts quality with forecast time is weaker for initialization times at the beginning of the night (typically 21UTC). For example, HR is typically 10% higher for simulations initialized at 21UTC and the FAR has the same behavior (Fig. 3). Consequently, predictions

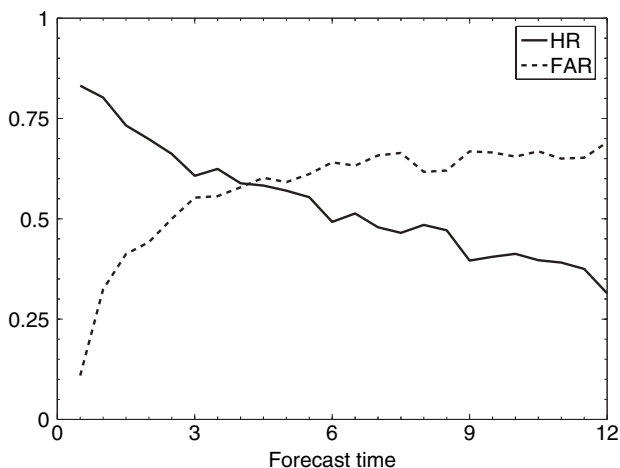


Figure 2

Cobel-Isba forecast of LVP conditions (all forecasts). Hit ratio (solid line) and false alarm rate (dashed line).

Table 1

Verification statistics of Cobel-Isba forecasts of LVP conditions for each initialization time at +1 h

	r00	r03	r06	r09	r12	r15	r18	r21	all
Good forecast	15	29	35	19	9	9	16	18	150
No detection	6	6	5	7	5	2	2	4	37
False alarm	19	9	12	10	3	5	5	9	72
HR	0.71	0.82	0.87	0.73	0.64	0.81	0.88	0.81	0.80
FAR	0.55	0.23	0.25	0.34	0.25	0.35	0.23	0.33	0.32

Table 2

Same as Table 1 at +3 h

	r00	r03	r06	r09	r12	r15	r18	r21	all
Good forecast	23	28	17	7	1	12	13	18	119
No detection	7	11	16	12	9	8	5	9	77
False alarm	29	27	27	14	7	9	16	18	147
HR	0.76	0.71	0.51	0.36	0.10	0.60	0.72	0.66	0.60
FAR	0.55	0.49	0.61	0.66	0.87	0.42	0.55	0.50	0.55

Table 3

Same as Table 1 at +6 h

	r00	r03	r06	r09	r12	r15	r18	r21	all
Good forecast	22	18	5	2	7	8	15	19	96
No detection	16	17	12	7	13	10	12	12	99
False alarm	27	28	17	9	4	14	28	34	171
HR	0.57	0.51	0.29	0.22	0.35	0.44	0.55	0.61	0.49
FAR	0.62	0.60	0.77	0.91	0.36	0.63	0.65	0.64	0.64

initialized at the beginning of the night could be successfully used to evaluate potential LVP occurrences during the night.

b. Accuracy on the Ceiling and Visibility Forecast

The LVP conditions are defined by ATC with two conditions: visibility less than 600 m or ceiling lower than 200 ft. Therefore, the quality of the Cobel-Isba forecast has also been evaluated for each of these individual conditions.

The frequency distribution histogram for observations and for the Cobel-Isba forecasts is plotted in Figure 4 for visibility lower than 600 m and in Figure 5 for ceiling lower than 200 ft. The distribution of the occurrence of visibility lower than 600 m is well forecasted by the Cobel-Isba model except for small differences between

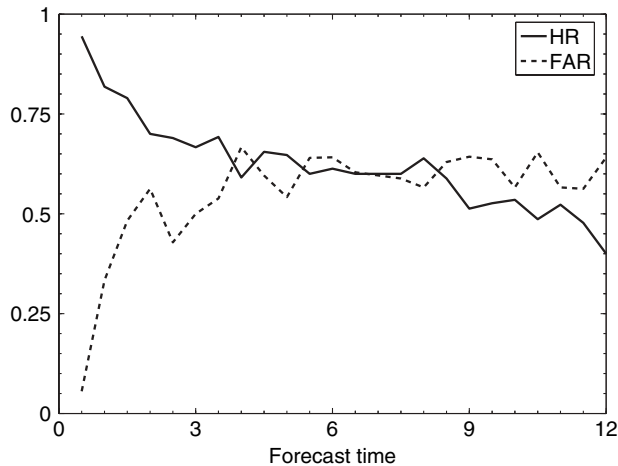


Figure 3

Same as Figure 2 for Cobel-Isba forecasts initialized at 21UTC.

08UTC and 10UTC. Cobel-Isba forecasts a slightly faster burn-off of fog at the beginning of the day (forecasted occurrence of 6.52% at 09UTC and 3.48% at 10UTC instead of observed occurrence of 5.65% at 09UTC and 3.77% at 10UTC). However, Figure 4 shows that the fog events are fairly well forecast by the Cobel-Isba model. The main differences between the Cobel-Isba forecast and observation appear more clearly on the low cloud cases (Fig. 5). The main weaknesses of the Cobel-Isba LVP forecasts previously shown in Figure 1 are observed again for low ceiling: over-forecast of low ceiling at the end of the night and under-forecast of low ceiling at the beginning of the night. This result indicates that the major weaknesses of the Cobel-Isba forecast are related to low clouds. This behavior has been previously determined by BERGOT *et al.* (2005) and seems to be a consequence of inaccurate mesoscale advections which are important to forecast low clouds (e.g., DRIEDONKS and DUYNKERKE, 1989).

NWP models, like Cobel-Isba, do not forecast horizontal visibility directly. Consequently, translation algorithms are required to compute visibility from prognostic variables. In Cobel-Isba, the visibility is deduced from the liquid water content alone following KUNKEL (1984). The observed visibility is compared to the forecasted visibility in Figure 6. The Cobel-Isba forecasts show a very rapid variation of the horizontal visibility, with visibility lower than 200 m for the majority of fog events. In contrast, the observed visibility is more scattered and the visibility occurrences lower than 200 m are small. This result demonstrates a tendency for the model to forecast a too dense fog and this problem points out inaccuracies in the microphysical parameterization and the crude quality of the diagnosed visibility. Currently, only the occurrence of fog can be forecast accurately by Cobel-Isba, and

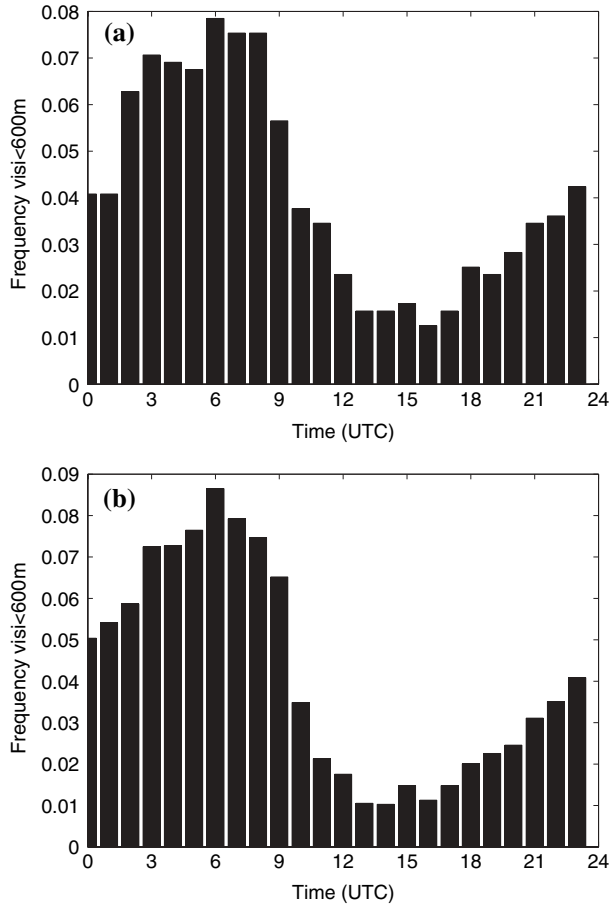


Figure 4

Frequency distribution histogram of visibility lower than 600 m as a function of daytime for observation (a), and Cobel-Isba forecasts (b).

not the value of the horizontal visibility inside the fog layer. An improved microphysical scheme and an improved translation algorithm seems to be required for accurately forecasting horizontal visibility. The histograms of low cloud ceiling plotted in Figure 7 show that the frequency of very low clouds (ceiling lower than 100 m) is quite well forecast. However, the presence of a ceiling lower than 500 m is overestimated. The rapid temporal variation of low clouds seems also not well forecast.

c. Accuracy of the Prediction of Onset and Burn-off Time

The anticipation of the beginning and end of LVP conditions is strategic for Air Traffic Control. Forecasting the beginning and the end time of LVP conditions is

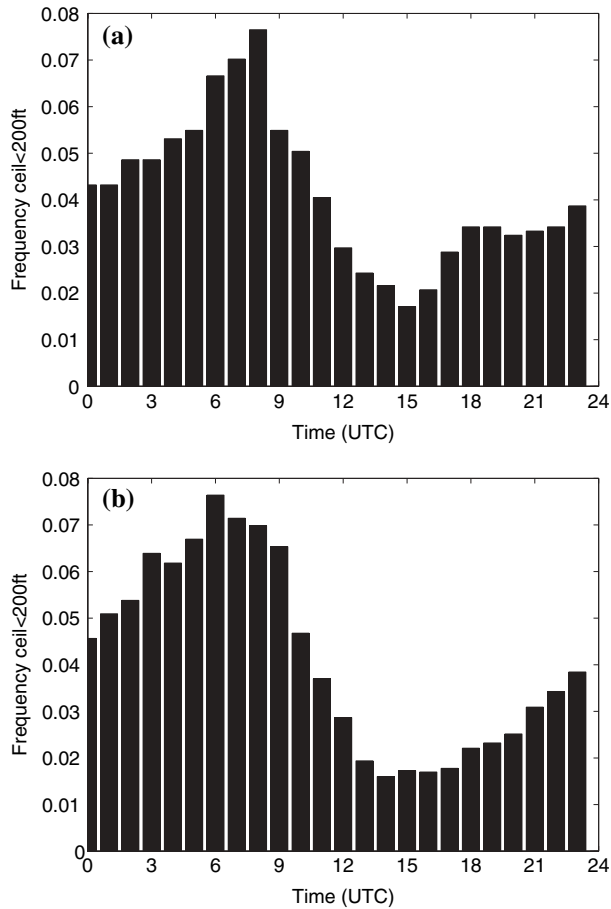


Figure 5
Same as Figure 4 for ceiling lower than 200 ft.

therefore identified as a priority. The error of forecast onset time is plotted in Figure 8, for forecast time up to +12 h. The error of onset time is unbiased, and the mean absolute error is about 1 h. The distribution of the onset error is relatively sharp: 55% of onset error time is less than 30 minutes and 63% is less than 1 hour. The error of the forecast end of LVP conditions is plotted in Figure 9. The error of burn-off time follows a bi-modal distribution, with two maxima at +1 h and -1 h error. The distribution is weakly biased (too late forecast of the end of LVP conditions of about 20 minutes), with a mean absolute error of about 1 hour 20 minutes. 27% of burn-off time error is less than 30 minutes, and 63% is less than 1 hour. The specific reason for this bi-modal distribution is unknown at this time, and unfortunately a more in-depth investigation is beyond the scope of this work.

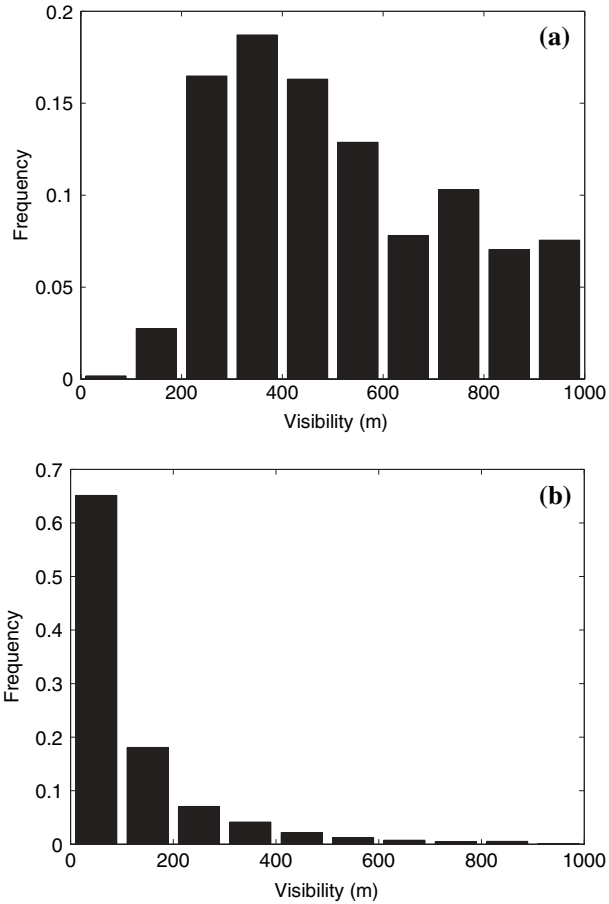


Figure 6

Frequency distribution histogram of the observed visibility (a), and forecast visibility (b).

The influence of aerosols (indirect effects and semi-direct radiative effects) on the burn-off time is suspected. The comparison between observations and the Cobel-Isba forecasts shows that the model has some skill in predicting LVP conditions for both onset and dissipation, with a typical error of 1 hour.

d. Influence of Meteorological Parameters

A systematic identification of the conditions that lead to forecast errors (no detection or false alarm) could be helpful for the operational use of the numerical LVP forecast at terminal airports. However, given the number of events, it is difficult to study each event and to draw conclusions. In order to simplify the identification of the errors, the number of well-forecast LVP events, the number of no detection and

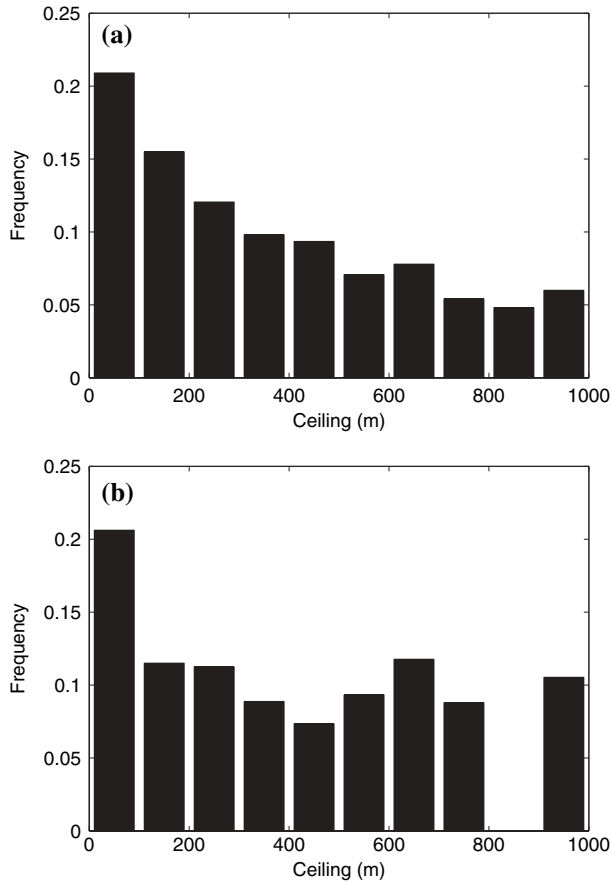


Figure 7
Same as Figure 6 for ceiling.

the number of false alarms have been classified as a function of the wind intensity, the wind direction and the surface pressure.

The Cobel-Isba forecasts of LVP conditions are more accurate for winds lower than 3 ms^{-1} (Fig. 10). An increase in the number of both no detection and false alarm is observed for wind between 3 ms^{-1} and 6 ms^{-1} . The lower winds mainly correspond to events dominated by local mechanisms, while mesoscale advections are more important for stronger winds. Consequently, the use of 1-D models is more fruitful in meteorological conditions with weak wind.

The dependence of the LVP forecast as a function of the wind direction is plotted in Figure 11. The forecasts are best for southeasterly wind, which mainly correspond to anticyclonic conditions. The false alarms are numerous for wind directions

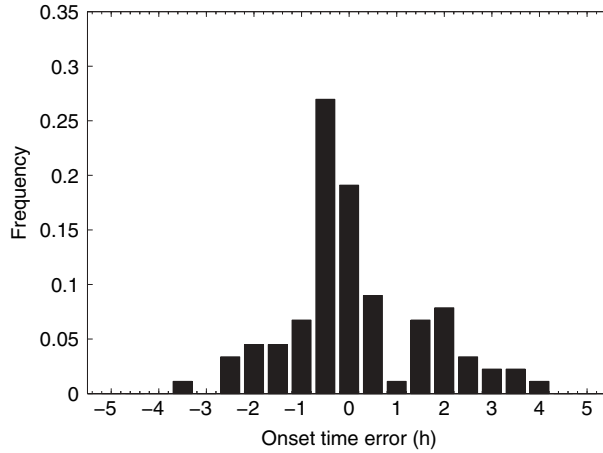


Figure 8

Frequency distribution histogram of the error on onset time (the LVP conditions at initial time are not taken into account). Positive values correspond to forecast of LVP onset that is too early.

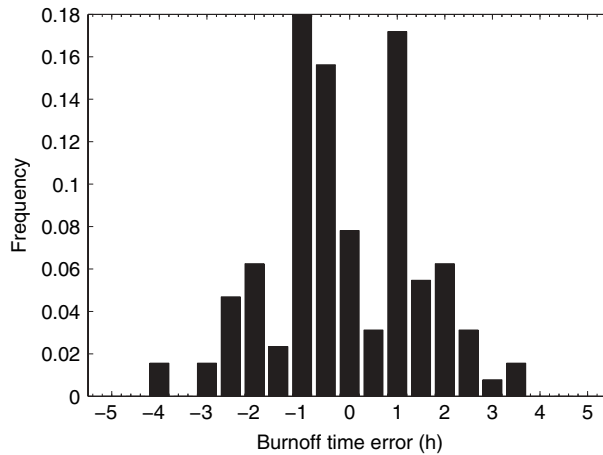


Figure 9

Frequency distribution histogram of the error on the end of LVP conditions. Positive values correspond to forecast of LVP burnoff that is too early.

between northwest and southwest. These directions mainly correspond to pre- or post-frontal conditions. In these meteorological situations, the mesoscale advections seem to prevent the occurrence of LVP conditions, and this effect seems poorly forecast by the Cobel-Isba model.

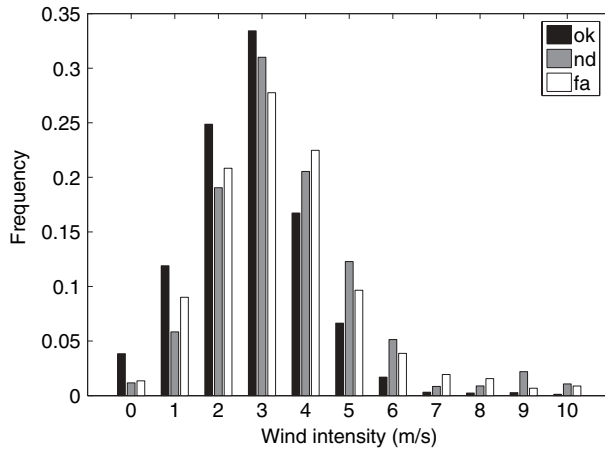


Figure 10

Frequency distribution histogram as a function of the wind intensity: Well forecast LVP events in black, no detection in gray and false alarm in white.

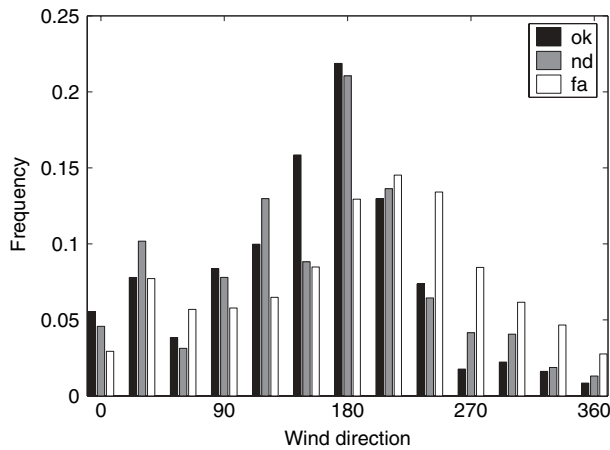


Figure 11

Same as Figure 10 for the wind direction.

The quality of the LVP forecast as a function of surface pressure is plotted in Figure 12. This figure confirms that LVP conditions in an anticyclonic situation are quite well forecast. conversely, when the surface pressure is lower than 1000 hPa, the number of errors (both no detection and false alarm) is relatively higher.

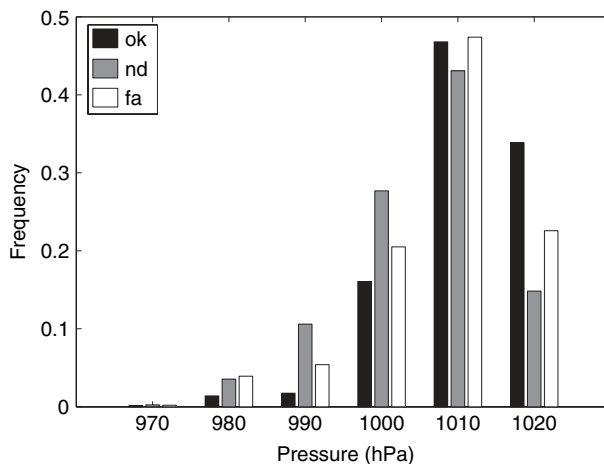


Figure 12
Same as Figure 10 for the surface pressure.

4. Conclusions

A local numerical method has been applied during three years to forecast fog and low clouds at Paris-CdG international airport. This numerical forecasting method is based on dedicated observations within the surface boundary layer, an adaptive assimilation scheme and the Cobel-Isba numerical model. This work provides a review of the performance of the Cobel-Isba numerical prediction system.

This study shows that the Cobel-Isba forecast of fog and low clouds is useful up to +6 h. During this forecast time, the false alarm rate is lower than the detection rate. The best results are obtained for 03UTC, 06UTC and 21UTC initialization times. The good results at the end of the night demonstrate the quality of the adaptive assimilation scheme associated with Cobel-Isba. The good quality of forecasts initialized at the beginning of the night demonstrates the quality of the Cobel-Isba numerical model to simulate the evolution of the nocturnal boundary layer. The major forecast weakness concerns the evolution of low clouds (stratus lowering). This result is confirmed by the study of the meteorological condition associated with errors. It seems that the low clouds are mainly driven by mesoscale flows and that the influence of the local conditions is weak. Therefore, it seems very difficult to accurately forecast the life cycle of low clouds with 1-D models.

This study has also evaluated the accuracy of the forecasts of the onset and end of fog events. For 63% of cases, the forecast errors on the onset or end of fog events are less than 1 h. This fact is very important because accurate anticipation of onset and cessation of foggy conditions provides the opportunity for Air Traffic Control to better regulate air traffic. Even if the occurrence of fog is well forecasted, the results

are not as encouraging for the forecast of the visibility in fog layers. This study reveals that the forecast visibility has a bias toward lower visibility than observed in fog. One way to improve the forecast of visibility would be to tune the translation algorithm and to improve the microphysics parameterization scheme.

These results are however very encouraging and show the usefulness of a forecast method based on a detailed local numerical model to forecast meteorological conditions at terminal airports. Given these encouraging results, the Cobel-Isba numerical forecast system is now integrated in the operational forecast system at Paris-CdG to provide a decision guidance tool.

The identification and understanding of the Cobel-Isba errors behavior open up the opportunity to reduce the impact of these errors on air traffic control. This could be accomplished through a systematic identification of the conditions that lead to these errors and then to indicate a weak predictability of these cases to end users. This work provides a basis for an optimal exploitation of the local numerical prediction system. Another way to estimate the predictability is to build an ensemble local prediction system. This research is described in ROQUELAURE and BERGOT (2007).

Acknowledgments

I would like to address many posthumous thanks to Peter Zwack for all the work performed on the Cobel model during numerous years, for his friendly help and for numerous discussions on the applications of the Cobel model. Many thanks to Robert Tardif for useful discussions and for his comments on an early version of this manuscript.

REFERENCES

- BERGOT, T. (1993), *Modélisation du brouillard à l'aide d'un mod. 1D forcé par des champs mésoéchelle: Application à la prévision*, Ph.D. Thesis, Université Paul Sabatier, Toulouse, France, 1546, 192 pp.
- BERGOT, T. and GUÉDALIA D. (1994), *Numerical forecasting of radiation fog. Part I: Numerical model and sensitivity tests*, *Mon. Wea. Rev.* 122, 1218–1230.
- BERGOT, T., CARRER, D., NOILHAN, J., and BOUGEALT, P. (2005), *Improved site-specific numerical prediction of fog and low clouds: A feasibility study*, *Weather and Forecasting* 20, 627–646.
- BOONE, A.A., Calvet, J.C., and Noilhan J. (1999) *The inclusion of a third soil layer in a land surface scheme using the force-restore method*. *J. Appl. Meteor.*, 38, 1611–1630.
- BOONE, A.A. (2000), *Modélisation des processus hydrologiques dans le schéma de surface ISBA: Inclusion d'un réservoir hydrologique, du gel et modélisation de la neige*, Ph.D. Thesis, Université Paul Sabatier, Toulouse, France, 252 pp.
- BOUGEALT, P. and LACARRERE, P. (1989), *Parameterization of orography-induced turbulence in a meso-scale model*, *Mon. Wea. Rev.* 117, 1872–1890.
- BROWN, R. and ROACH, W.T. (1976), *The physics of radiation fog. Part II: A numerical study*, *Quart. J. Roy. Meteorol. Soc.* 102, 335–354.

- CLARK, D.A. (2002), *The 2001 demonstration of automated cloud forecast guidance products for San Francisco international airport*, Proc. 10th Conf. on Aviation, Range, and Aerospace Meteorology, AMS.
- CLARK, D.A. (2006), *Terminal ceiling and visibility product development for northeast airports*, Proc. 14th Conf. on Aviation, Range, and Aerospace Meteorology, AMS.
- DRIEDONKS, A.G.M. and DUYNKERKE, P.G. (1989), *Current problem in the strato-cumulus topped atmospheric boundary layer*, Bound. Layer Meteor. 46, 275–303.
- DUYNKERKE, P.G. (1991), *Radiation fog: A comparison of model simulation with detailed observations*, Mon. Wea. Rev. 119, 324–341.
- ESTOURNEL, C. and GUEDALIA, D. (1987), *A new parameterization of eddy diffusivities for nocturnal boundary layer modeling*, Bound. Layer. Meteor. 39, 191–203.
- FOUQUART Y. and BONNEL, B. (1980), *Computations of solar heating of the Earth's atmosphere: A new parameterization*, Beitr. Phys. Atmosph. 53, 35–62.
- GULTEPE, I. (2005), *A new warm fog microphysical parameterization developed using aircraft observations*, Proc. COST722 Workshop on “short-range Forecasting Methods of Fog, Visibility and Low Clouds,” ESF, 46–57.
- HERZEGH, P.H., BENJAMIN, S.G., RASMUSSEN, R., TSUI, T., WIENER, G., and ZWACK, P. (2003), *Development of automated analysis and forecast products for adverse ceiling and visibility conditions*, Proc. 19th Internat. Conf. on Interactive Information and Processing Systems for Meteorology, Oceanography and Hydrology, AMS, 8–13 Feb., Long-Beach, California, U.S.A.
- KUNKEL, B. (1984), *Parameterization of droplet terminal velocity and extinction coefficient in fog model*, J. Appl. Meteor. 23, 34–41.
- MUSSON-GENON, L. (1986), *Numerical simulation of a fog event with a one-dimensional boundary layer model*, Mon. Wea. Rev. 115, 592–607.
- NOILHAN J. and PLANTON, S. (1989), *A simple parameterization of land surface processes for meteorological models*, Mon. Wea. Rev. 117, 536–549.
- ROQUELAURE, S. and BERGOT, T. (2007), *Seasonal sensitivity on COBEL-ISBA local forecast system for fog and low clouds*, Pure Appl. Geophys. 164, 6/7, (this issue).
- TARDIF, R. (2007), *The impact of vertical resolution in explicit numerical forecasting of radiation fog: A case study*, Pure Appl. Geophys. 164, 6/7, (this issue).
- TERRADELLAS, E. and Cano, D. (2003), *Implementation of a one-dimensional model for local forecasts at Madrid airport*, Proc. EGS-AGU-EGU Joint Assembly, ESF.
- TERRADELLAS, E. and GLOWACKA, A., CANO, D. (2005), *The use of measured temperatures in the initialisation of 1-D model developed for fog forecast*, Proc. COST722 workshop on “Short-range Forecasting Methods of Fog, Visibility and Low Clouds,” ESF, 58–62.
- VEHIL, R., MONNERIS, J., GUEDALIA, D. and SARTHOU P. (1989), *Study of radiative effects (longwave and shortwave) within a fog layer*, Atmos. Res. 23, 179–194.

(Received March 23, 2006, accepted August 5, 2006)

Published Online First: June 8, 2007

To access this journal online:
www.birkhauser.ch/pageoph
